Molecular Model for Light-Driven Spiral Mass Transport in Azopolymer Films

Antonio Ambrosio,[1,*] Pasqualino Maddalena,[1,2] and Lorenzo Marrucci[1,2,†]

[1]*CNR-SPIN, Complesso Universitario di Monte Sant'Angelo, 80126 Napoli, Italy*

[2]*Dipartimento di Fisica, Università di Napoli "Federico II," Complesso Universitario di Monte Sant'Angelo, 80126 Napoli, Italy*

(Received 23 January 2013; published 5 April 2013)

Azopolymer films exposed to nonuniform illumination exhibit a phenomenon of light-induced mass transport, leading to the formation of permanent relief patterns on the film surface. Its underlying microscopic mechanism remains unclear, despite many years of research effort. Here we introduce a model of the mass migration process based on anisotropic light-driven molecular diffusion. A key ingredient of our model is an enhanced molecular diffusion in proximity of the free polymer surface, which is essential for explaining, in particular, the recently observed spiral-shaped reliefs resulting from vortex-beam illumination.

DOI: 10.1103/PhysRevLett.110.146102 PACS numbers: 68.55.am, 68.35.bm, 82.30.Qt, 82.50.Hp

When a polymer containing azobenzene side chains or separate molecular dopants is irradiated with visible or ultraviolet light, its molecules undergo several light-induced processes of rearrangement. In particular, an effective reorientation of the azobenzene moieties is induced, in connection with *trans-cis-trans* isomerization cycles or related photoinduced effects [1–4]. In addition, a light-driven molecular migration—or mass transport—takes place, leading to the creation of stable reliefs and valleys on the polymer surface, while keeping the total polymer volume approximately constant [5,6]. These reliefs form patterns that are related in a nontrivial way with the illuminating field structure [7–9]. The mass transport appears to occur preferentially in the direction of the electric field and to result from a photoinduced fluidization of the material [9–13]. These optical writing phenomena make azopolymers very attractive for optical data storage applications or for the nanoscale imaging of electromagnetic field distribution [14,15]. Recently, the potential advantage of using azopolymers in the place of sacrificial photoresists in the fabrication of silicon micro- and nanostructures has also been demonstrated [13,16].

A complete understanding of the microscopic mechanism underlying the mass-transport process is still lacking [13]. Proposed models for the optical driving force range from light-induced internal stresses resulting from the *trans-cis* isomerization and associated variations of the molecular mean occupied volume [17,18], to dielectric or dipolar field-gradient forces [19–21], to mean-field forces arising from the anisotropy of molecular interactions [22], to photoinduced anisotropic molecular diffusion or random-walk effects [23–26]. All these models, however, share a common feature: they ultimately link the light-induced mass-transport action to gradients of the optical field. This is indeed what occurs in most illumination experiments. However, nothing in these models could apparently predict a dependence of the light-induced mass transport on the wave front structure of the writing beam. Yet, in Ref. [27], we have reported an unexpected sensitivity of the mass transport to the helical wave front handedness of a writing laser beam with an optical vortex on its axis, i.e., carrying orbital angular momentum (OAM) (see, e.g., Ref. [28] for a recent review on this kind of optical beams). This sensitivity is highlighted, in particular, by the spiral-shaped structure of the resulting relief pattern, as shown, for example, in Fig. 1(a), with the spiral handedness responding to the optical vortex one [27].

In order to explain this surprising observation, we have developed a symmetry-based phenomenological model

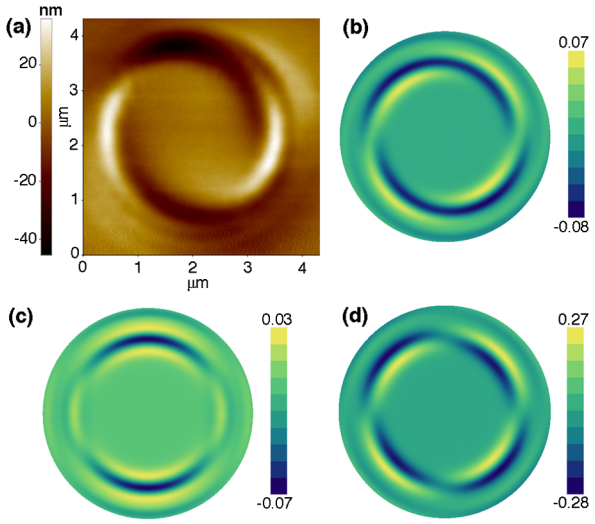

FIG. 1 (color online). Relief spiral patterns induced on the polymer by an impinging vortex light beam having orbital angular momentum eigenvalue and vortex charge $q = 20$. (a) Experimental results, imaged using an atomic force microscope. (b) Pattern predicted by our model for the optimal value of the ratio $c_S/c_2 = 4/\lambda$ (with $c_1/c_2 = c_3/c_2 = -0.15$). (c) Pattern predicted by our model for $c_S = 0$ (vanishing surface effect). (d) Pattern predicted by our model for $c_S/c_2 = 16/\lambda$ (very strong surface effect). The simulated pattern height scale is in arbitrary units.

that includes a new surface-related term in the light-driven mass current, depending on the optical field but independent of its gradients, which explains the main qualitative features of the observed relief patterns [27]. However, the phenomenological model introduced in Ref. [27] was not linked to any specific microscopic mechanism and in principle might be compatible with different options. In this Letter we go one step further and propose a detailed microscopic mechanism, consistent with our previous phenomenological model, that provides a first complete picture of the wave front-sensitive light-induced mass transport phenomenon. Moreover, in order to compare our model with experiment, in this Letter we report additional experimental results on the relief patterns induced by vortex light illumination, in particular, for vortex charge $q = 20$, higher than all previously investigated cases. All details about the experimental layout and the polymer material can be found in Ref. [27].

As we shall see, our model is mainly built on the light-induced anisotropic diffusion concept [23–25], which is, however, combined with additional assumptions on the role of the polymer surface in favoring the diffusion. The microscopic model we present here is oversimplified in many respects, but we believe that it captures some essential features of the molecular mechanism underlying the phenomenon. A complete quantitative model should presumably have to complement these basic features with a more detailed description of molecular correlations and orientational order, at a microscopic level, and of the effects of viscoelastic response of the polymer, at a more macroscopic level.

Let us then consider a polymer thin film deposited on a rigid substrate and initially extending in the region comprised between the plane $z = 0$ (interface with the substrate) and the plane $z = L$ (free surface). After exposure to light, the polymer develops surface reliefs, which can be described by the surface height variations $\Delta h(x, y)$ as a function of the transverse coordinates x, y. We assume that these surface reliefs arise as a consequence of light-induced mass transport, as described by a mass-current-density vector $\mathbf{J}$. The link between the mass current vector and the height variations, as derived from a standard incompressibility assumption and a thin-film approximation (see Ref. [27] for details), is given by the following expression:

$$\Delta h(x, y) = -\frac{L\Delta t}{\rho}\partial_k \bar{J}_k, \quad \text{with} \quad k = x, y, \tag{1}$$

where Δt is the irradiation time, ρ is the polymer mass density, ∂_k denotes the partial derivative with respect to the transverse coordinates x, y (sum over repeated indices is understood), and $\bar{\mathbf{J}} = (\int_0^L \mathbf{J} dz)/L$ is the mass current averaged across the film thickness L.

In the following, for simplicity we shall refer to the azo chromophore of the polymer as it were an individual molecule. Each azo molecule shall be characterized by its position $\mathbf{r}$ and by the orientation of its main axis, as indicated by a unit vector $\hat{\boldsymbol{\mu}}$. Let us denote with $n(\mathbf{r}, \hat{\boldsymbol{\mu}})$ the number density of azo molecules per unit volume and solid angle. The molecular axis $\hat{\boldsymbol{\mu}}$ plays two independent roles in our model. The first is that of defining the direction of the molecular transition dipole moment involved in the light absorption. Therefore, the excitation probability per unit time of a molecule can be written as follows:

$$p(\mathbf{r}, \hat{\boldsymbol{\mu}}) = \alpha |\hat{\boldsymbol{\mu}} \cdot \mathbf{E}(\mathbf{r})|^2, \tag{2}$$

where $\mathbf{E}(\mathbf{r})$ is the (complex) optical electric field and α is a constant proportional to the absorption coefficient at the irradiation wavelength λ. If we assume that the fraction of excited molecules is small (an assumption that is always valid, for sufficiently small light intensity) and that molecular rearrangements (displacements and rotations) taking place during each excitation cycle are small, then the number density of excited molecules per unit volume and solid angle can be approximately written as $n_e(\mathbf{r}, \hat{\boldsymbol{\mu}}) = p(\mathbf{r}, \hat{\boldsymbol{\mu}})\tau_e n(\mathbf{r}, \hat{\boldsymbol{\mu}})$, where τ_e is the excited state lifetime. See the Supplemental Material for more details [29].

The second role of the molecular axis $\hat{\boldsymbol{\mu}}$ in our model is that of defining the direction along which the molecule may perform a short random walk during its excited lifetime, as in the warmlike motion of azo molecules first proposed in Ref. [23]. The one-dimensional mass current (per unit volume and solid angle) resulting from this random walk can be expressed mathematically by the following expression:

$$J(\mathbf{r}, \hat{\boldsymbol{\mu}}) = -D(z)\frac{dn_e}{dx_\mu} = -D(z)\hat{\boldsymbol{\mu}} \cdot \boldsymbol{\nabla} n_e(\mathbf{r}, \hat{\boldsymbol{\mu}}), \tag{3}$$

where $D(z)$ is a molecular diffusion constant, which we take here to depend on z. In particular, we shall assume this constant to be uniform $D(z) = D_B$ in the polymer bulk, while close to the polymer surface it changes to a possibly different surface value $D(L) = D_S$. At the interface with the substrate we instead assume the diffusion constant to vanish, $D(0) = 0$, so that this interface cannot contribute to the mass transport.

In order to evaluate Eq. (3), we must first calculate the molecule distribution $n(\mathbf{r}, \hat{\boldsymbol{\mu}})$. Here we make another important approximation; i.e., we assume that this distribution can be simply replaced with the equilibrium one, neglecting all light-induced effects on it. This assumption actually corresponds again to a lowest-order (quadratic) approximation in the optical field, because a quadratic factor in the field is already present in the excitation probability p appearing in the excited-state distribution n_e that ultimately determines the molecular current. Therefore, all dependences of the distribution n on the field will only contribute to higher-order terms in the field. Of course, for intense or prolonged illuminations this lowest-order approximation will fail, and a more

sophisticated solution will be needed. At equilibrium, molecule position and orientation can be considered as approximately uncorrelated variables, and hence we can write $n(\mathbf{r}, \hat{\boldsymbol{\mu}}) = N(\mathbf{r})f(\hat{\boldsymbol{\mu}})$, where $N(\mathbf{r})$ is the molecular number density and $f(\hat{\boldsymbol{\mu}})$ is the orientational distribution. Assuming a uniform distribution of azo molecules in the polymer film, the first is then written as $N(\mathbf{r}) = N_0\theta(z)\theta(L-z)$, where N_0 is the (uniform) bulk number density and $\theta(z)$ is the Heaviside step function [i.e., $\theta(z) = 0$ for $z < 0$ and $\theta(z) = 1$ for $z > 0$], here used to describe, in an abrupt approximation, the polymer surface located at $z = L$ and the interface with the substrate located at $z = 0$. The equilibrium molecule orientational distribution is taken to be isotropic; that is, $f(\hat{\boldsymbol{\mu}}) = 1/(4\pi)$. This assumption is certainly valid at the beginning of the irradiation. During the irradiation, the molecules will reorient randomly and after many excitations will tend to become orthogonal to the electric field, so they become anisotropically distributed. However, as already explained above, this effect leads to higher-order terms in the optical field, which we neglect here.

We are now ready to write an expression for the excited molecule distribution:

$$n_e(\mathbf{r}, \hat{\boldsymbol{\mu}}) = \frac{\alpha\tau_e N_0}{4\pi}|\hat{\boldsymbol{\mu}}\cdot\mathbf{E}(\mathbf{r})|^2\theta(z)\theta(L-z). \quad (4)$$

Inserting this expression into Eq. (3), we can calculate the 1D current density

$$J(\mathbf{r}, \hat{\boldsymbol{\mu}}) = -\frac{\alpha\tau_e N_0}{4\pi}D(z)\{\theta(z)\theta(L-z)\hat{\boldsymbol{\mu}}\cdot\boldsymbol{\nabla}[|\hat{\boldsymbol{\mu}}\cdot\mathbf{E}(\mathbf{r})|^2] + [\delta(z-L)-\delta(z)](\hat{\boldsymbol{\mu}}\cdot\hat{\mathbf{z}})|\hat{\boldsymbol{\mu}}\cdot\mathbf{E}(\mathbf{r})|^2\}, \quad (5)$$

where we have introduced the surface normal unit vector $\hat{\mathbf{z}}$ and Dirac's delta function $\delta(z)$. The first term appearing within curly brackets in this expression of the current is a bulk term, in which the gradients leading to the current are due to the nonuniform light illumination only. The second term, with the δ functions, can be interpreted as interfacial terms with currents driven by the rapid variation of molecule concentration. Since we have assumed $D(z) = 0$ for $z = 0$, we can drop the second of these interfacial terms (relative to the interface with the substrate) and retain only the surface term, for $z = L$.

The transverse current density $\bar{\mathbf{J}}$ can now be obtained by integrating over the entire solid angle and averaging along z across the film thickness (assuming z-independent optical fields), as shown in detail in the Supplemental Material [29]. After these steps, we obtain

$$\bar{J}_k = C_1\partial_k(E_l^*E_l) + C_2\partial_l(E_l^*E_k + E_k^*E_l) + C_3\partial_k|E_z|^2 + \frac{C_S}{L}(E_z^*E_k + E_zE_k^*), \quad \text{with} \quad k, l = x, y, \quad (6)$$

with

$$C_1 = C_2 = C_3 = -\frac{\alpha\tau_e N_0 D_B}{15}, \quad C_S = \frac{\alpha\tau_e N_0 D_S}{15}. \quad (7)$$

Inserting Eq. (6) into Eq. (1), we obtain the following final expression for the pattern of surface reliefs or valleys (see also the Supplemental Material [29] for an equivalent but more explicit expression in terms of the field Cartesian components):

$$\Delta h(x, y) = c_1\partial_k\partial_k(E_l^*E_l) + c_2\partial_k\partial_l(E_l^*E_k) + c_3\partial_k\partial_k|E_z|^2 + 2c_S\partial_k\mathrm{Re}(E_z^*E_k) \quad \text{with} \quad k, l = x, y, \quad (8)$$

where

$$c_1 = c_3 = -\frac{L\Delta t C_1}{\rho} = \frac{L\Delta t\alpha\tau_e N_0 D_B}{15\rho}, \quad c_2 = -\frac{2L\Delta t C_2}{\rho} = 2c_1, \quad c_S = -\frac{\Delta t C_S}{\rho} = -\frac{\Delta t\alpha\tau_e N_0 D_S}{15\rho}. \quad (9)$$

The results given in Eqs. (6) and (8) are perfectly consistent with those of our phenomenological model [27,30]. We remark that the first three terms in Eqs. (6) and (8) refer to bulk effects, while the fourth is an additional surface-related effect. The latter vanishes identically for most illumination geometries investigated in the past, but it does not vanish for certain particular illumination patterns, such as the vortex beam case.

In contrast with a phenomenological analysis, a microscopic model provides expressions for the coefficients appearing in the constitutive equations in terms of molecular properties. We can then use the experimental data to estimate the value of these unknown molecular quantities. In particular, with our experimental values [27], we obtain the following order of magnitude estimates: $D_B\tau_e \sim 10^{-43}$ kg m^2. For a typical lifetime $\tau_e \sim 10$ ps and our polymer mass per azo molecule of $m_A = 325$ Da, one obtains $D_B/m_A \sim 2\times10^{-8}$ m^2/s and a single random-walk step of $\sqrt{D_B\tau_e/m_A} \sim 4$ Å. These values are reasonable and consistent with previously reported estimates [23], although they imply a surprisingly good efficiency of the process.

Another interesting prediction of our model concerns the relative values of the four terms appearing in Eq. (8), which can be readily compared with the results of experiments. In particular, in Ref. [27], we have experimentally estimated a ratio $|c_S/c_2| \approx 4/\lambda$, which corresponds to $|C_S/C_2| \approx 10$, in order to explain the spiral relief shape. In Fig. 1 we show how the simulated pattern loses its spiral shape for smaller and larger values of this ratio (although the variation is very slow, and this implies a high uncertainty on the reported optimal value). This in turn implies that $D_S/D_B \approx 10$; i.e., the molecule light-driven mobility is enhanced close to the surface by about 1 order of magnitude (the random-walk step is increased by a factor of 3), which is a reasonable result, considering that the number of polymer entanglements will be strongly reduced at the surface.

Another prediction of our model is $C_1 = C_2 = C_3$, leading to $c_2 = 2c_1 = 2c_3$. The coefficient c_1 controls a mass-transport current along the gradient of light intensity regardless of polarization, while c_2 corresponds to the additional transport effect occurring when the light gradient is parallel to the optical electric field (c_3 gives a mass transport controlled by the intensity of the longitudinal component of the electric field, so it is usually less relevant). The role of these two factors is best understood in a simpler irradiation geometry, such as with the interference fringes created by two plane waves impinging on the sample obliquely at two opposite incidence angles. The induced relief pattern in such experiments is a grating, similar to the writing interference pattern [5,6], and this is also predicted by our model (see supplemental information of Ref. [27]). However, the amplitude of the relief modulation depends on the polarization of the interfering beams. Let us consider the two main optical polarization geometries, ss and pp, corresponding to an optical electric field that is, respectively, perpendicular and parallel to the incidence plane (and hence to the resulting field gradient). Our model predicts a relief modulation amplitude proportional to c_1 in the ss case and to $c_1 + c_2$ in the pp case. Hence, the predicted ratio of these two amplitudes is $c_1/(c_1 + c_2) = 1/3$. This value does not agree with the results of most experiments, for which an ss illumination generates barely visible relief gratings, much smaller than the pp ones [9,10,24]. Hence, the mass motion seems to take place almost exclusively along the light electric field, which in our model corresponds to setting $c_1 \ll c_2$.

A similar discrepancy is found in the case of single Gaussian beam illumination. Assuming a coefficient ratio $c_1/(c_1 + c_2) = 1/3$ leads to the modulated ring relief pattern shown in Fig. 2(c), with a maximum ring height in the direction of the polarization (vertical in the figure) and a minimum in the perpendicular (horizontal) direction. The ratio between these minimum and maximum heights is just $1/3$. Similar ring patterns were obtained in previous numerical simulations (see, e.g., Fig. 2 in Ref. [25] and Fig. 2 in Ref. [26]). However, the experimental patterns look different, as shown in Fig. 2(a) (see also previous experiments [7,8]): there is no visible relief in a direction perpendicular to the polarization, again consistent with a mass motion taking place only along the light electric field. In our model, this corresponds again to setting $c_1 \ll c_2$. Actually, the optimal agreement is obtained for slightly negative values, i.e., $c_1/c_2 = c_3/c_2 \approx -0.15$, as shown in Fig. 2(b) [31].

We ascribe these discrepancies between the experiment and the predictions of our microscopic model mainly to our lowest-order approximation in the optical field. Most experiments are indeed performed in a nonlinear regime, in which the light-induced orientational effects are strong and faster than the mass transport ones. Therefore, azo molecules tend to reorient perpendicular to the light polarization relatively quickly, and then stop absorbing and moving. This "orientational bleaching" can be counteracted by the mass transport when the latter occurs parallel to the optical electric field, because the polymer dragging will tend to realign the azo molecules again parallel to the field. Instead, an initial mass transport perpendicular to the electric field makes the bleaching even faster and quickly leads the process to a complete stop. Strong evidence in favor of this qualitative explanation is provided by other experiments in which an incoherent uniform "assisting beam" with orthogonal polarization is used to "recycle" the molecules into a random orientation (but without contributing to the mass transport), thus preventing them from reaching this orientational bleaching [32,33].

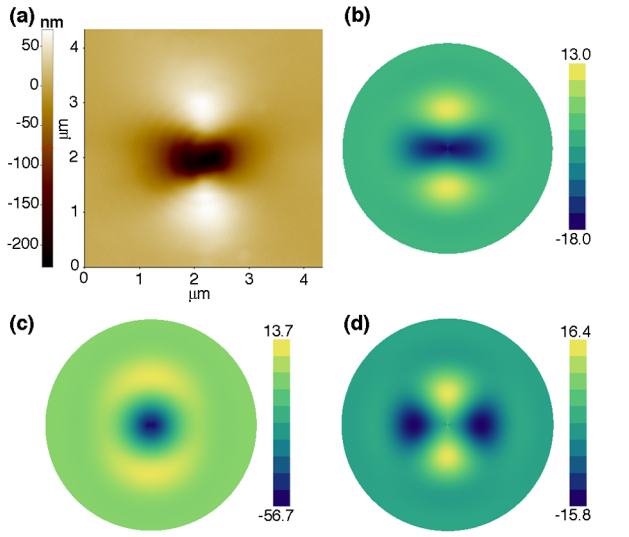

FIG. 2 (color online). Relief patterns induced on the polymer by an impinging Gaussian light beam (i.e., vortex charge $q = 0$). (a) Experimental results, imaged using an atomic force microscope. (b) Pattern predicted by our model, for $c_1/c_2 = -0.15$ (optimal value). (c) Pattern predicted by our model for $c_1/c_2 = 0.5$. (d) Pattern predicted by our model for $c_1/c_2 = -0.5$. In all simulations, we assumed $c_3 = c_1$. The simulated pattern vertical scale is in arbitrary units.

In conclusion, our model provides a realistic, although simplified, description of the light-induced mass-transport process at the molecular scale, illustrating the microscopic nature of the surface-enhanced diffusion term needed to explain the spiral relief patterns observed under vortex light illumination. However, in order to correctly predict the ratio between the different coefficients appearing in the light-induced mass current, the role of molecular orientational order (and probably also the viscoelastic response of the polymer) will need to be included in the model.

We acknowledge the support of the European Commission, 7th Framework Programme, under Grants No. 264098, MAMA and No. 255914, PHORBITECH, the latter within the Future Emerging Technologies FET-Open programme.

*antonio.ambrosio@spin.cnr.it
†marrucci@na.infn.it

[1] T. Todorov, L. Nikolova, and N. Tomova, Appl. Opt. **23**, 4309 (1984).
[2] M. Eich, J. H. Wendorff, B. Reck, and H. Ringsdorf, Makromol. Chem. Rapid Commun. **8**, 59 (1987).
[3] A. Natansohn and P. Rochon, Chem. Rev. **102**, 4139 (2002).
[4] C. Manzo, D. Paparo, and L. Marrucci, Phys. Rev. E **70**, 051702 (2004).
[5] P. Rochon, E. Batalla, and A. Natansohn, Appl. Phys. Lett. **66**, 136 (1995).
[6] D. Y. Kim, S. K. Tripathy, L. Li, and J. Kumar, Appl. Phys. Lett. **66**, 1166 (1995).
[7] S. Bian, L. Li, J. Kumar, D. Y. Kim, J. Williams, and S. K. Tripathy, Appl. Phys. Lett. **73**, 1817 (1998).
[8] S. Bian, J. M. Williams, D. Yu Kim, L. Li, S. Balasubramanian, J. Kumar, and S. Tripathy, J. Appl. Phys. **86**, 4498 (1999).
[9] N. K. Viswanathan, D. Y. Kim, S. Bian, J. Williams, W. Liu, L. Li, L. Samuelson, J. Kumar, and S. K. Tripathy, J. Mater. Chem. **9**, 1941 (1999).
[10] P. Karageorgiev, D. Neher, B. Schulz, B. Stiller, U. Pietsch, M. Giersig, and L. Brehmer, Nat. Mater. **4**, 699 (2005).
[11] A. Ambrosio, A. Camposeo, P. Maddalena, S. Patanè, and M. Allegrini, J. Microsc. **229**, 307 (2008).
[12] A. Ambrosio, E. Orabona, P. Maddalena, A. Camposeo, M. Polo, A. A. R. Neves, D. Pisignano, A. Carella, F. Borbone, and A. Roviello, Appl. Phys. Lett. **94**, 011115 (2009).
[13] S. Lee, H. S. Kang, and J.-K. Park, Adv. Mater. **24**, 2069 (2012).
[14] R. Bachelot *et al.*, J. Appl. Phys. **94**, 2060 (2003).
[15] H. Ishitobi, M. Tunabe, Z. Sekkat, and S. Kawata, Appl. Phys. Lett. **91**, 091911 (2007).
[16] A. Kravchenko, A. Shevchenko, V. Ovchinnikov, A. Priimagi, and M. Kaivola, Adv. Mater. **23**, 4174 (2011).
[17] C. J. Barrett, P. L. Rochon, and A. Natansohn, J. Chem. Phys. **109**, 1505 (1998).
[18] D. Bublitz, B. Fleck, and L. Wenke, Appl. Phys. B **72**, 931 (2001).
[19] J. Kumar, L. Li, X. L. Jiang, D.-Y. Kim, T. S. Lee, and S. Tripathy, Appl. Phys. Lett. **72**, 2096 (1998).
[20] K. Sumaru, T. Fukuda, T. Kimura, H. Matsuda, and T. Yamanaka, J. Appl. Phys. **91**, 3421 (2002).
[21] K. Yang, S. Yang, and J. Kumar, Phys. Rev. B **73**, 165204 (2006).
[22] T. G. Pedersen, P. M. Johansen, N. C. R. Holme, P. S. Ramanujam, and S. Hvilsted, Phys. Rev. Lett. **80**, 89 (1998).
[23] P. Lefin, C. Fiorini, and J.-M. Nunzi, Pure Appl. Opt. **7**, 71 (1998).
[24] B. Bellini, J. Ackermann, H. Klein, Ch. Grave, Ph. Dumas, and V. Safarov, J. Phys. Condens. Matter **18**, S1817 (2006).
[25] M. L. Juan, J. Plain, R. Bachelot, P. Royer, S. K. Gray, and G. P. Wiederrecht, Appl. Phys. Lett. **93**, 153304 (2008).
[26] M. L. Juan, J. Plain, R. Bachelot, P. Royer, S. K. Gray, and G. P. Wiederrecht, ACS Nano **3**, 1573 (2009).
[27] A. Ambrosio, L. Marrucci, F. Borbone, A. Roviello, and P. Maddalena, Nat. Commun. **3**, 989 (2012)
[28] A. M. Yao and M. J. Padgett, Adv. Opt. Photonics **3**, 161 (2011).
[29] See Supplemental Material at http://link.aps.org/supplemental/10.1103/PhysRevLett.110.146102 for a more detailed derivation of the model results.
[30] We note that c_S is here defined so that $c_S = c_B = c'_B/2$ where c_B and c'_B are those defined in the supplemental information of Ref. [27], while the symbol c_B appearing in the main article of Ref. [27] includes an additional factor 2.
[31] In Ref. [27] we reported $c_1 \approx c_3 \approx 0$, but we had not included negative values in the test range.
[32] K. Yang, S. Yang, X. Wang, and J. Kumar, Appl. Phys. Lett. **84**, 4517 (2004).
[33] F. Fabbri, Y. Lassailly, S. Monaco, K. Lahlil, J. P. Boilot, and J. Peretti, Phys. Rev. B **86**, 115440 (2012).